Supporting Information

Lice Yu[a], Shuli Wang[a], Yun Yang*[b] and Ligang Feng*[a]

a School of Chemistry and Chemical Engineering, Yangzhou University, Yangzhou, 225002, PR China. Email: ligang.feng@yzu.edu.cn; fenglg11@gmail.com (L Feng*)

b Nanomaterials and Chemistry Key Laboratory, Wenzhou University, Wenzhou, China. E-mail: bachier@163.com

1. Experimental section

1.1. Materials and chemicals

N, N-dimethylformamide (DMF), molybdenyl acetylacetonate ($C_{10}H_{14}MoO_6$), palladium chloride ($PdCl_2$) and sodium hypophosphite (NaH_2PO_2) were purchased from Shanghai Aladdin Biochemical Technology Co., Ltd. Polyacrylonitrile (PAN, Mw=150000) and 5 wt.% Nafion ionomers were obtained from Sigma-Aldrich. Sodium hydroxide, methyl alcohol, ethyl alcohol, vitriol, hydrochloric acid, and potassium chloride were purchased from Sinopharm Chemical Reagent Co., Ltd. All the chemicals in this study were analytical grade and used without purification. Ultrapure water with a resistance of 18.2 MΩ (Thermo Fisher Scientific Co., LTD, USA) was used throughout all experiments.

1.2. Materials fabrication

1.2.1. Synthesis of MoP carbon nanofiber (MoP@CNF)

1 g PAN was dissolved into 10 mL DMF solvent, followed by the addition of 3 mmol $C_{10}H_{14}MoO_6$. After magnetic stirring at room temperature for 12 hours, the mixture solution was loaded into a 10 mL syringe for electrospinning. Then the precursor solution was subsequently electro spun at a feeding rate of 0.012 mL min^{-1} and a high voltage of 20 kV. The distance between the injector nozzle and the receiver was 15 cm, and the PAN-$C_{10}H_{14}MoO_6$ nanofibers were collected on the aluminum-foil paper. The above composite nanofibers were thermally treated in the air atmosphere at 260 ^oC for 2 h with a heating rate of 1 ^oC min^{-1} for pre-oxidation to stabilize the as-spun nanofibers and avoid cracks and defects, then it was further phosphatized at 900 ^oC in the N_2 atmosphere for 2 h with a heating rate of 2 ^oC min^{-1} in a tube furnace to improve the carbonization degree and conductivity. Finally, MoP@CNF were obtained.

1.2.2. Preparation of Pd/MoP@CNF catalyst

A certain amount of MoP@CNF was dispersed in 50 mL ethylene glycol by ultra sonification for 20 min to form a uniform suspension. $PdCl_2$ solution containing 20 mg Pd was added in the process, and then the pH of the suspension was adjusted to about 11.0 with 1.0 M NaOH solution. The suspension was placed in a 700 W microwave oven for 60 s, and the operation was repeated three times to get the catalyst. The suspension was naturally cooled to room temperature and centrifuged several times, and then the Pd/MoP@CNF was collected (about 100 mg). Pd/CNF catalyst of 20 wt% was prepared by the above method and carbon nanofibers were used to replace

MoP@CNF.

1.3 Physical characterizations

The XRD was implemented by Bruker D8 advance X-ray diffraction with Cu Kα radiation. The morphologies and structural characterizations were investigated by scan electron microscopy (SEM, FEI Sirion-200). Transmission electron microscopy (TEM), high-resolution transmission electron microscopy (HRTEM), high-annular dark-field scanning transmission electron microscopy (STEM) and element mapping analysis were conducted on FEI TECNAI G2 electron microscope operating at 200 kV. X-ray photoelectron spectroscopy (XPS) measurements were carried on an ECSALAB250Xi S3 spectrometer with an Al Kα radiation source. X-ray detector spectrum (EDX) images were obtained on a TECNAI G2 F30 transmission electron microscope (acceleration voltage: 300 kV). Inductively coupled plasm atomic emission spectroscopy (ICP-AES) analysis was carried out on Optima 7300 DV.

1.4 Electrochemical Pre-treatment

All the electrochemical measurements were conducted in a conventional three-electrode system controlled by a Bio-Logic VSP electrochemical workstation (Bio-Logic Co., France). The graphite rod and the saturated calomel electrode (SCE, Hg/Hg_2Cl_2) worked as the counter and reference electrode. It is worth noting that the reference electrode was carefully calibrated and checked before and after the test to ensure its accuracy.

The performance of various catalysts was evaluated by coating the catalyst over the glassy carbon electrode. The catalyst ink was prepared by ultrasonically dispersing a mixture containing 2.5 mg catalyst, 475 μL of ethanol, and 25 μL of a 5 wt.% Nafion solution. Then 10 μL of the catalyst ink was pipetted and dropped onto the precleaned glassy carbon electrode with the geometric surface area of 0.07 cm^2 and dried at room temperature, the catalyst loading on the glassy carbon electrode: 0.40 mg cm^{-2}. All of the potentials were relative to the SCE electrode.

1.5 Electrochemical analysis of formic acid electrooxidation (FAEO)

1.5.1 Cyclic voltammetry test

The activity of metal nanoparticles for formic acid electro-oxidation was measured. Before electrochemical measurements, a nitrogen flow was bubbled into the test system to remove the oxygen, and ad/desorption of hydrogen on metal nanoparticles surface was evaluated in 0.5 M H_2SO_4. Cyclic voltammetry (CV) was carried out at room temperature in 0.5 M H_2SO_4 + 0.5 M

HCOOH solution at a potential range between -0.2 and 1.0 V vs. SCE and at the scan rate of 20 mV s^{-1}.

1.5.2 Stability test

The chronoamperometry (CA) experiments were performed in 0.5 M H_2SO_4 and 0.5 M HCOOH solution at 0.1 V vs. SCE for 3600 s to estimate the stability of the catalysts for formic acid oxidation.

1.5.3 CO stripping test

For formic acid oxidation, 99.99 % CO was subsequently bubbled in the 0.5 M H_2SO_4 for 15 min when the potential was controlled to be 0 V vs. SCE. The excess CO in the electrolyte was purged out with N_2 for 15 min. The CO stripping was performed in the potential of the range -0.2 ~ 1.0 V vs. SCE at 20 mV s^{-1}. The electrochemical surface area (ECSA) and the tolerance to CO poisoning were estimated by the CO stripping test. The ECSA values were calculated from the equation:

ECSA=Q/Sl.

Where Q is the coulombic charge (in mC) obtained from the CO stripping curve. l is the loading of Pd on the surface of the electrode (in mg) and S is a proportionality constant of 420 mC cm^{-2}.

1.5.4 Tafel analysis

The Tafel slope was calculated from the following equation: $\eta = a + b \log (j)$, $b = 2.3*RT/\alpha F$, where η is the overpotential (mV), a represents the intercept, j stands for the current density and b defines the Tafel slope. R, T, α, F refer to gas constant, temperature, charge transfer coefficient, and Faraday constant, respectively. α can reflect the intrinsic property of electron transfer; the larger the value, the better the electrochemical dynamics.

1.5.5 Electrochemical impedance measurements

The electrochemical impedance spectra (EIS) were recorded at the frequency range from 1000 kHz to 30 mHz with 12 points per decade. The amplitude of the sinusoidal potential signal was 5 mV. The obtained curves were analyzed and fitted by ZsimpWin computer program.

1.6 Electrochemical analysis of hydrogen evolution reaction

For hydrogen evolution reaction (HER), all potentials were converted and referred to the reversible hydrogen electrode (RHE): E (RHE) = E (SCE) + 0.059*pH + 0.242 V.

1.6.1 Cyclic voltammetry test

The catalytic performance of catalysts for HER was evaluated by CV curves at a scan rate of 5 mV s^{-1} with the potential scan range from -0.158 to 0.242 V.

1.6.2 Stability test

The CA experiment of HER was tested in -0.036 V for 10 h in 0.5 M H_2SO_4 + 0.5 M HCOOH solution.

1.6.3 Tafel analysis

The analytical method was consistent with the above formic acid oxidation reaction.

1.6.4 Electrochemical impedance measurements

The EIS were recorded at the frequency range from 1000 kHz to 10 mHz with 15 points per decade in 0.5 M H_2SO_4 + 0.5 M HCOOH solution.

1.7 Electrochemical analysis of two-electrode electrolysis

For two-electrode electrolysis, the ink of catalysts was both used as the anode and cathode, respectively. The CV curves were tested in 0.5 M H_2SO_4 with and without 0.5 M HCOOH at a scan rate of 5 mV s^{-1} with the potential scan range from 0 to 2.0 V. The CA test of the two-electrode was tested in 0.63 V for 10 h in 0.5 M H_2SO_4 + 0.5 M HCOOH solution.

2. Theoretical calculation section

The CASTEP module of the Materials Studio software (Accelrys Inc.) was employed for the quantum chemistry calculations. Perdew−Burke−Ernzerh (PBE) of approximation was selected as the generalized gradient approximation (GGA) method to calculate the exchange-correlation energy. The Broyden−Fletcher−Goldfarb−Shanno (BFGS) scheme was selected as the minimization algorithm. The energy cut off is 560 eV and the SCF tolerance is 1.0×10^{-6} eV/atom. The optimization is completed when the energy, maximum force, maximum stress and maximum displacement are smaller than 1.0×10^{-6} eV/atom, 0.01 eV/Å, 0.02 GPa and 5.0×10^{-4} Å, respectively. A vacuum slab exceeding 15 Å was employed in the z direction to avoid the interaction between two periodic units.

In addition, it should be noted that the DFT calculation of supported catalysts was mainly devoted to study the intrinsic activity of the catalyst and its mechanism of action in the catalytic reaction, without consideration of the atomic ratio of the constructed catalyst. When calculating the Gibbs free energy, we mainly explored the intrinsic activity of a single active site in different catalysts to avoid the influence of noble metal content on the results.

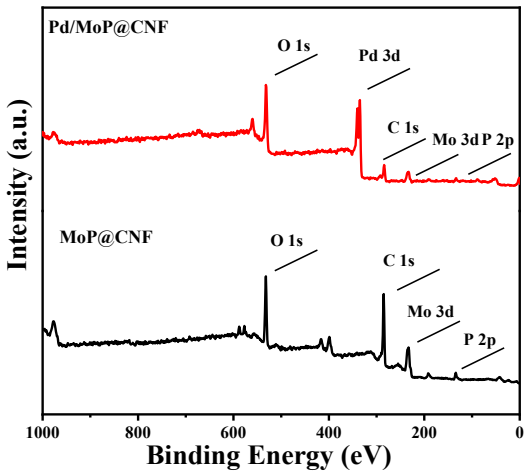

Figure S1. XPS survey scan spectrum of Pd/MoP@CNF and MoP@CNF.

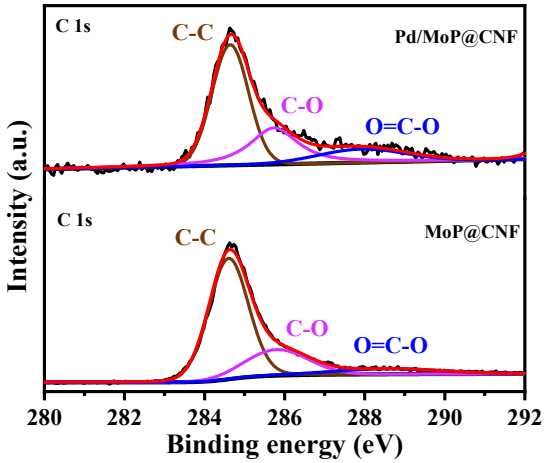

Figure S2. XPS spectra of C1s of Pd/MoP@CNF and MoP@CNF catalysts.

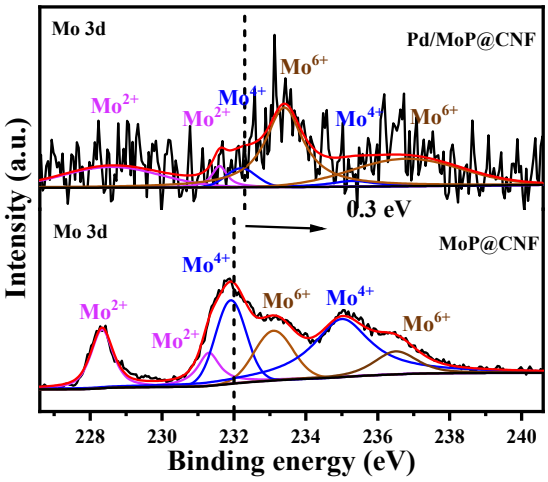

Figure S3. The XPS spectra of the Mo 3d region for Pd/MoP@CNF and MoP@CNF.

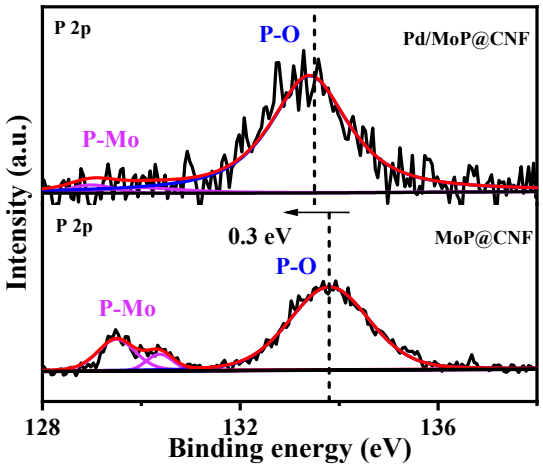

Figure S4. The XPS spectra of the P 2p region for Pd/MoP@CNF and MoP@CNF.

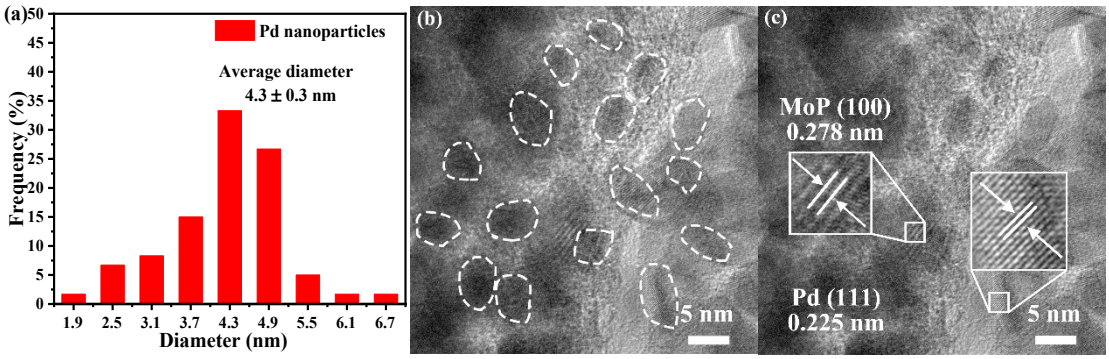

Figure S5. (a) The particle size distribution histogram of Pd nanoparticles on the Pd/MoP@CNF surface; (b-c) TEM image of Pd/MoP@CNF.

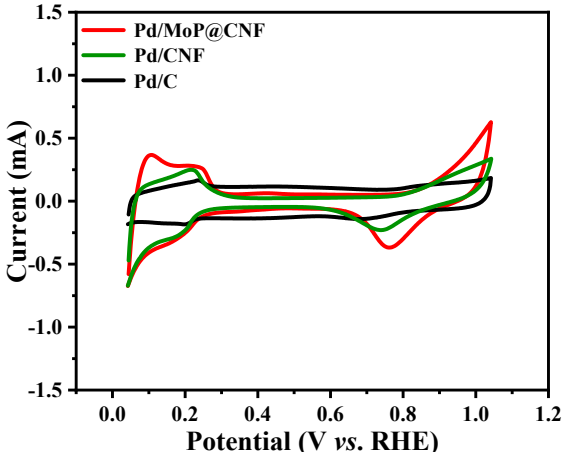

Figure S6. Cyclic voltammetry curves of Pd/MoP@CNF, Pd/CNF and Pd/C in N_2-purged 0.5 M H_2SO_4 solution at a scan rate of 50 mV s^{-1}.

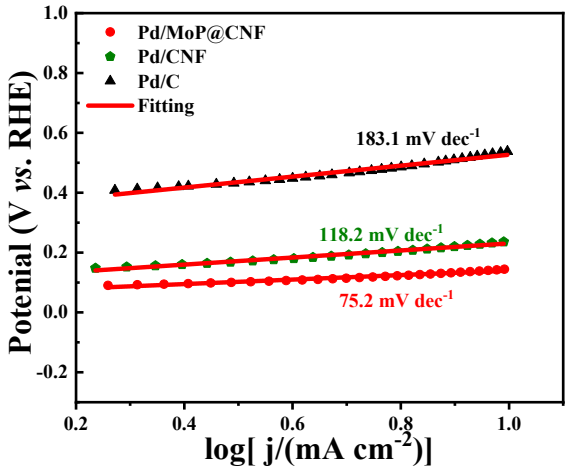

Figure S7. The corresponding Tafel plots of Pd/MoP@CNF, Pd/CNF and Pd/C catalysts for formic acid oxidation.

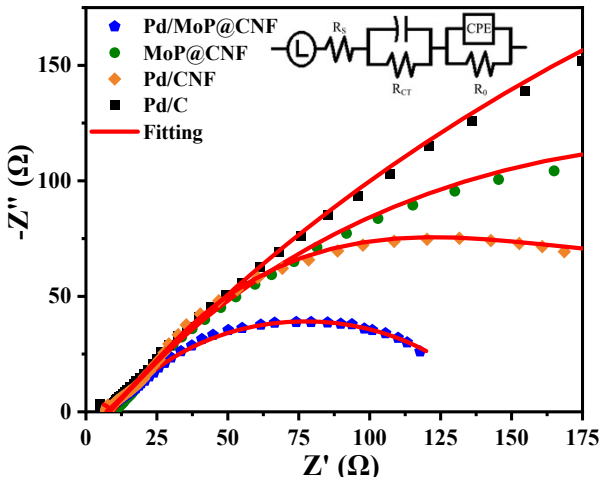

Figure S8. The Nyquist plots of Pd/MoP@CNF, MoP@CNF, Pd/CNF and Pd/C catalysts for formic acid oxidation (inset: equivalent circuit).

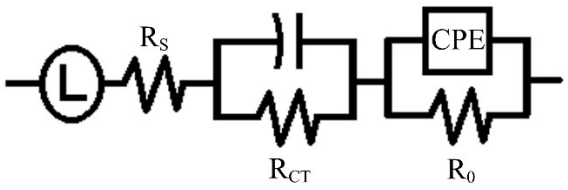

Figure S9. For the equivalent circuit, L comes from the inductance of an external circuit without electrochemical process involved; other physical components have general meaning in which R_s is a signal of uncompensated solution resistance, R_{ct} represents the charge transfer resistance and R_0 is the contact resistance between the catalyst and the electrode, and two solid-phase elements (CPE)

constitute a double-layer capacitor.

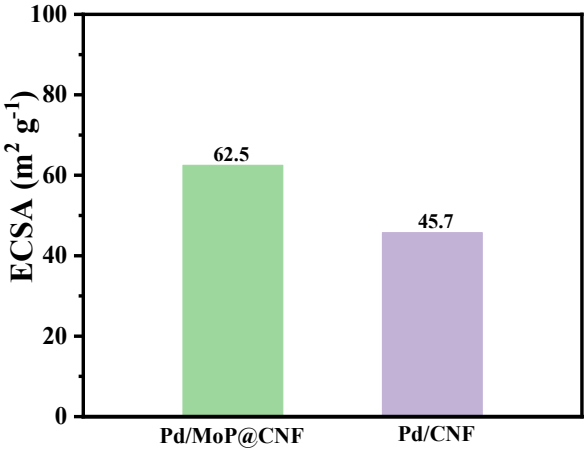

Figure S10. The electrochemical surface area of Pd/MoP@CNF and Pd/CNF.

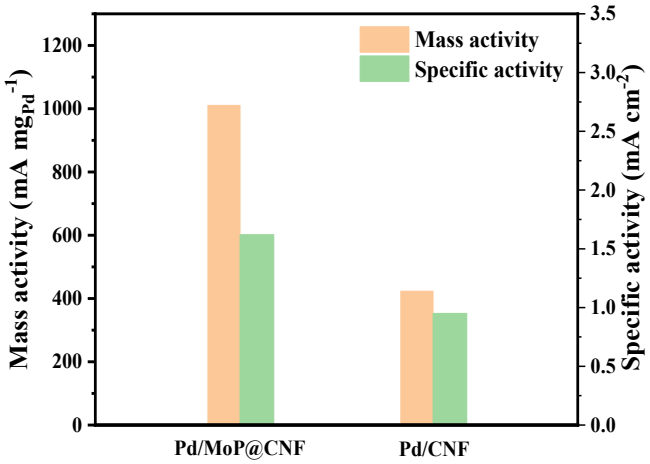

Figure S11. Mass activity and specific activity of Pd/MoP@CNF and Pd/CNF in N_2-purged 0.5 M H_2SO_4 + 0.5 M HCOOH solution at a scan rate of 20 mV s^{-1}.

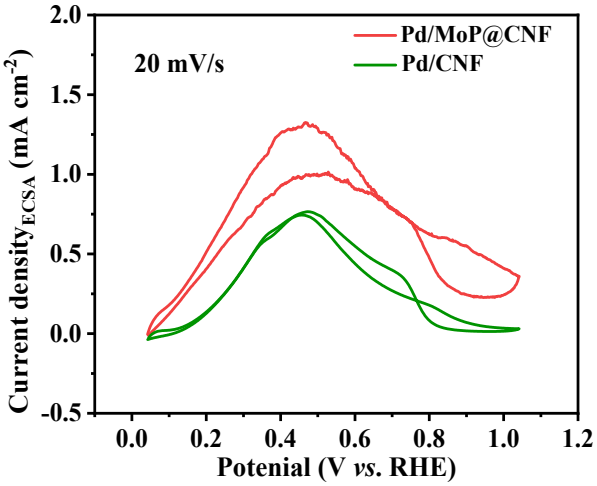

Figure S12. Specific activity of Pd/MoP@CNF and Pd/CNF catalysts in N_2-purged 0.5 M H_2SO_4 + 0.5 M HCOOH solution at a scan rate of 20 mV s^{-1}.

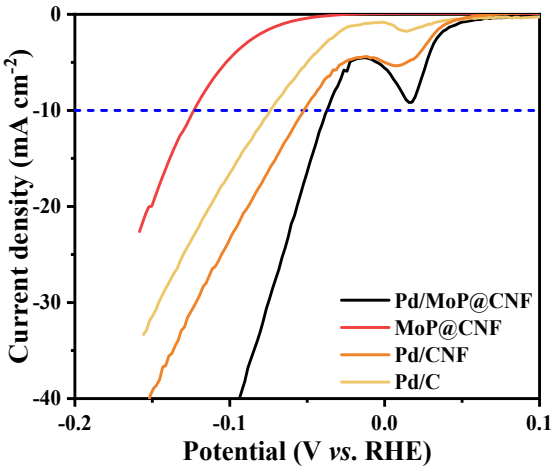

Figure S13. HER polarization curves of Pd/MoP@CNF, MoP@CNF, Pd/CNF and Pd/C catalysts at 5 mV s^{-1}.

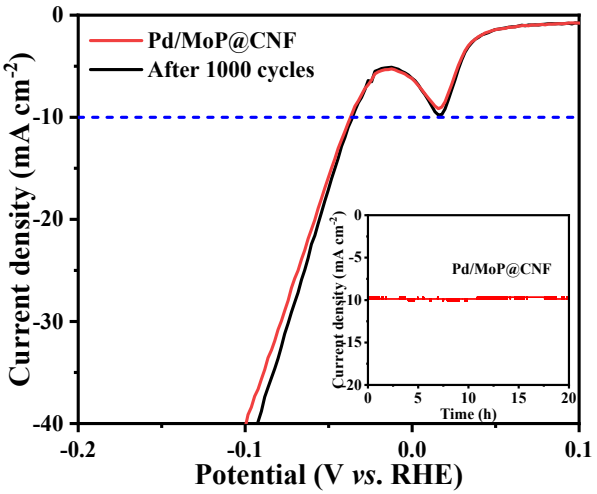

Figure S14. HER polarization curves before and after 1000 CVs of Pd/MoP@CNF (inset: chronoamperometry curve for Pd/MoP@CNF in 0.5 M H_2SO_4 + 0.5 M HCOOH solution at -0.036 V vs. RHE for 20 h).

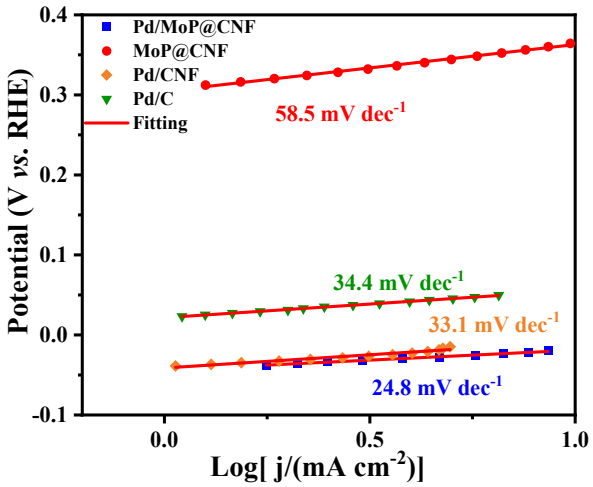

Figure S15. Tafel slope of Pd/MoP@CNF, MoP@CNF, Pd/CNF and Pd/C catalysts in 0.5 M H_2SO_4 + 0.5 M HCOOH solution.

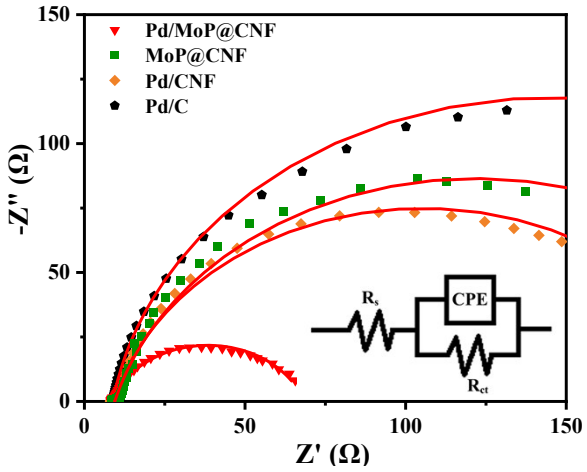

Figure S16. Nyquist plots of Pd/MoP@CNF, MoP@CNF, Pd/CNF and Pd/C catalysts for HER at -0.036 V vs. RHE (inset: equivalent circuit).

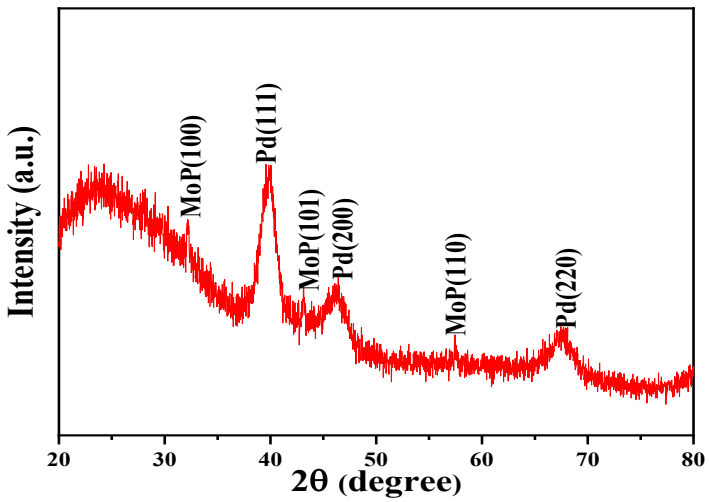

Figure S17. The XRD pattern of Pd/MoP@CNF after long-term stability tests for FAEO.

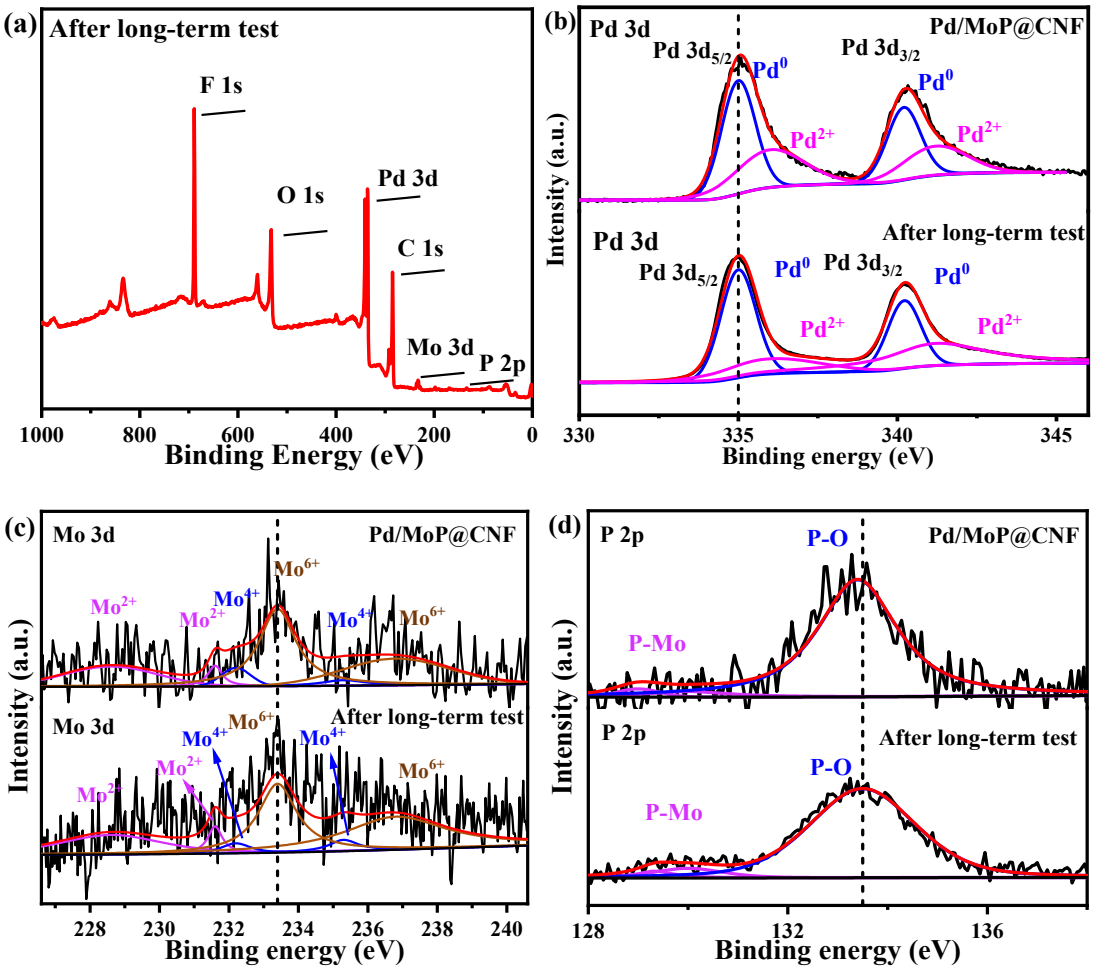

Figure S18. XPS of Pd/MoP@CNF after long-term stability tests for FAEO.

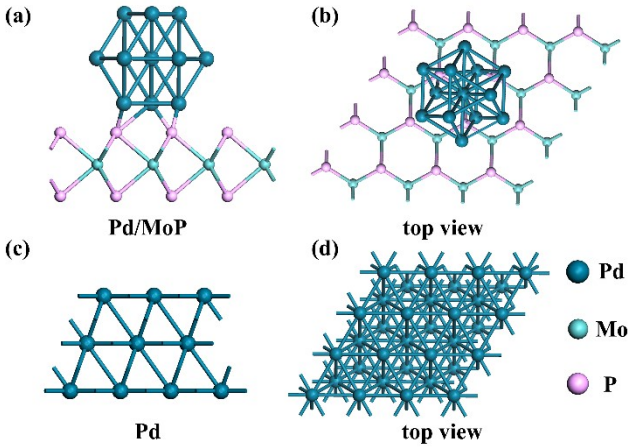

Figure S19. The model of (a-b) Pd/MoP and (c-d) Pd from front and top view.

Table S1. The binding energy of the Pd $3d_{5/2}$ and Pd $3d_{3/2}$ components for Pd/MoP@CNF and Pd/CNF.

Catalysts	Pd $3d_{5/2}$		Pd $3d_{3/2}$		Content	Pd (0)/ Pd (+2)
	Peak	Binding energy (eV)	Peak	Binding energy (eV)		
Pd/MoP@CNF	Pd (0)	335.0	Pd (0)	340.2	57.8 %	1.4
	Pd (+2)	336.0	Pd (+2)	341.2	42.2 %	
Pd/CNF	Pd (0)	335.5	Pd (0)	340.7	51.6 %	1.1
	Pd (+2)	336.5	Pd (+2)	341.7	48.4 %	

Table S2. The binding energy of the Mo $3d_{5/2}$ and Mo $3d_{3/2}$ components for Pd/MoP@CNF and MoP@CNF.

Catalysts	Mo $3d_{5/2}$		Mo $3d_{3/2}$		Content
	Peak	Binding energy (eV)	Peak	Binding energy (eV)	
Pd/MoP@CNF	Mo (+2)	228.6	Mo (+2)	231.6	22.7%
	Mo (+4)	232.2	Mo (+4)	235.3	8.0%
	Mo (+6)	233.4	Mo (+6)	236.8	69.3%
MoP@CNF	Mo (+2)	228.3	Mo (+2)	231.3	20.9%
	Mo (+4)	231.9	Mo (+4)	235.0	55.9%
	Mo (+6)	233.1	Mo (+6)	236.5	23.2%

Table S3. Mass fraction of each element from the ICP-AES and EDX data.

Catalyst	Pd (%)	Mo (%)	P (%)
Pd/MoP@CNF (ICP-AES)	17.6	38.9	10.2
Pd/MoP@CNF (EDX)	18.2	39.8	12.2

Table S4. EIS fitting parameters from equivalent circuits for different catalyst samples in 0.5 M H_2SO_4 + 0.5 M HCOOH for formic acid oxidation.

Material	R_s/Ω	CPE-Yo/S $_S^{-n}$	CPE-n	C/F	R_{ct}/Ω	L/H	R_0/Ω	Chi squared
Pd/MoP@CNF	8.0	1.0E-3	0.7	1.6E-4	133.8	1.9E-13	2.5	6.8E-3
MoP@CNF	7.4	2.1E-3	0.6	2.1E-8	350.4	3.6E-20	53.9	4.6E-3
Pd/CNF	7.2	2.3E-3	0.5	7.9E-4	268.8	5.1E-9	61.3	7.3E-3
Pd/C	6.6	2.1E-3	0.6	1.6E-9	482.4	4.7E-15	5.8	2.2E-3

Table S5. EIS fitting parameters from equivalent circuits for different catalyst samples in 0.5 M H_2SO_4 + 0.5 M HCOOH for hydrogen evolution.

Material	R_s/Ω	CPE-Yo/S $_S^{-n}$	CPE-n	R_{ct}/Ω	Chi squared
Pd/MoP@CNF	8.5	1.1E-3	0.8	59.8	8.1E-4
MoP@CNF	9.4	6.8E-4	0.8	224.8	7.3E-3
Pd/CNF	9.1	7.5E-4	0.8	192.6	6.4E-3
Pd/C	8.9	1.7E-5	0.9	274.4	1.5E-3